Quantum interference in the spectrum of a driven atom: Effects of pumping and phase fluctuations

A. H. Toor,* S.-Y. Zhu, and M. S. Zubairy*
Department of Physics, Hong Kong Baptist University, Hong Kong
(Received 19 May 1995)

The quantum interference in the spontaneous-emission spectrum of a driven atom, when the upper level of the atomic transition is coupled to a third level via a classical driving field, results in a dark line in the absence of the atomic decays. The existence of the dark line is independent of the Rabi frequency associated with the driving field. There is no such dark line in the spontaneous-emission spectrum when, instead of the upper level, the lower level is coupled to a third level via a driving field. In this paper, we include the level decays, incoherent pumping, and the finite bandwidth of the driving field in our analysis and study their role in the spontaneous-emission spectrum in the two configurations.

PACS number(s): 42.50.−p

I. INTRODUCTION

The interaction of an excited atom with the vacuum results in the spontaneous emission of the radiation. This radiation has an isotropic distribution in space which leads to a Lorentzian linewidth in the frequency domain with the bandwidth proportional to the Einstein spontaneous decay rate [1]. In the well-studied problem of resonance fluorescence, where a two-level atom is driven by a strong field, this Lorentzian spectrum splits into a three-peak spectrum [2]. In this three-peak spectrum, the location of the peaks is governed by the Rabi frequency of the driving field whereas the widths of these peaks are determined by the Einstein spontaneous decay rate. Recently, Narducci *et al.* [3] have predicted that an additional coupling to a third level in an excited atom in the resonance fluorescence configuration would lead to significantly different results for the spontaneous-emission spectrum and, under certain conditions, spectral narrowing in the resonance fluorescence spectrum is obtained. These results have been experimentally verified [4].

A closely related, but much older, problem is the so-called Autler-Townes spontaneous emission from a driven atom. If one of the two levels involved in the spontaneous emission is coupled by a strong coherent field to another level, the spontaneous-emission spectrum is a two-peak distribution known as the Autler-Townes doublet [5]. Recently, Zhu, Narducci, and Scully [6] have pointed out a dark line in the Autler-Townes spontaneous-emission spectrum when the excited level is coupled to a third level via a classical field. The existence of the dark line is independent of the Rabi frequency associated with this driving field. No such dark line is present when, instead of the excited level, the ground level is coupled to another level via a classical field. In a simple model, which did not include any level decays, they showed that the presence of a dark line in the spontaneous-emission spectrum of an upper driven atom is due to the quantum interference in the two possible paths. This is an example of a number of novel phenomena associated with quantum interference in driven three-level systems which include absorption cancellation [7], correlated spontaneous-emission laser [8], lasing without inversion [9], electromagnetically induced transparency [10], and enhancement of the index of refraction with no absorption [11].

It would be interesting to see, especially from an experimentalist's point of view, how the spontaneous-emission spectrum from a driven atom is modified when the level decays, the incoherent pumping, and the finite bandwidth of the driving field are included in the analysis. In this paper we present analytical results for the spontaneous-emission spectra in both upper- and lower-level coupling configurations when all the level decays, pumping rates, and the finite bandwidth of the driving field are included and discuss our results with reference to the quantum interference in the three-level system. The finite bandwidth of the driving field is incorporated by taking into account the phase fluctuations associated with the driving field [12]. In our model, these phase fluctuations lead to a Lorentzian linewidth of the driving field. Above threshold, the amplitude and phase fluctuations are decoupled and for a well-stabilized laser, the amplitude fluctuations can be neglected. A comparison between the results for the spontaneous-emission spectrum for the two schemes (upper- and lower-level couplings) indicates the presence of a much larger dip in the spectrum of the upper coupling case as opposed to a much smaller dip in the case of lower coupling. Our results elucidate the conditions under which this dip corresponding to a dark line in the spontaneous-emission spectrum can be experimentally observed.

II. MODEL

We consider two possible schemes in which the spontaneous-emission spectrum of an excited atomic state decaying to the ground state is effected by a coupling with an additional atomic level. We consider the spontaneous emission in a three-level atom. In the first scheme, an arbitrarily strong classical field, having a finite bandwidth, couples the excited level with the additional level [see Fig. 1(a)], whereas in the second scheme a driving field induces a coupling between the ground level and the additional atomic

*Permanent address: Department of Electronics, Quaid-i-Azam University, Islamabad 45320, Pakistan.

1050-2947/95/52(6)/4803(9)/$06.00 © 1995 The American Physical Society

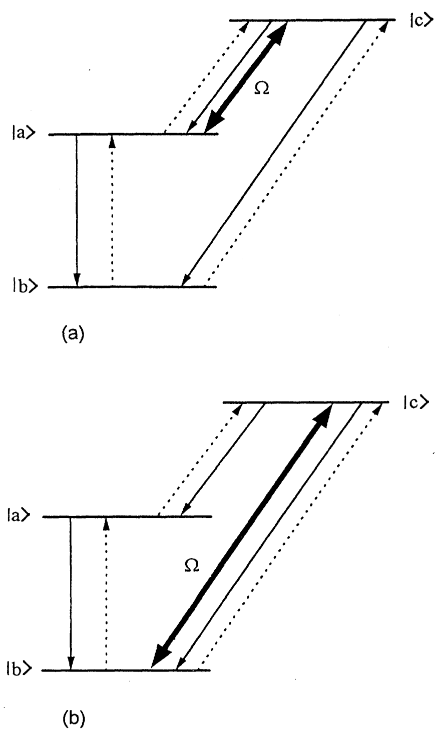

FIG. 1. Schematic representation of two atomic configurations: (a) upper-level coupling scheme, (b) lower-level coupling scheme. The arrows with dotted lines indicate the incoherent pumpings and those with solid line represent the atomic decay from one level to another.

level [see Fig. 1(b)]. We shall refer to the two schemes as the upper-level coupling and the lower-level coupling scheme, respectively. In both the schemes, we include appropriate level decays and incoherent pumps in a closed system configuration.

A. Upper-level coupling scheme

In this scheme, a classical field is driving the upper level $|a\rangle$ of a three-level atomic system [see Fig. 1(a)]. In the presence of this additional coupling with level $|c\rangle$, the atomic level $|a\rangle$ spontaneously decays to the ground level $|b\rangle$. The phase of the driving field is fluctuating, which leads to the finite bandwidth. In the following, we calculate the spontaneous-emission spectrum from atomic level $|a\rangle$.

The Hamiltonian for the system, in the interaction picture and under the rotating-wave approximation, can be written as

$$V_{\rm int}=-\hbar\Delta|c\rangle\langle c|-\hbar\left[\frac{\Omega}{2}e^{-i\phi(t)}|c\rangle\langle a|+\frac{\Omega^*}{2}e^{i\phi(t)}|a\rangle\langle c|\right], \tag{1}$$

where Ω is the induced Rabi frequency and $\phi(t)$ is the time-dependent fluctuating phase of the field driving the upper two atomic levels. The detuning between the atomic transition frequency of the upper two atomic levels, i.e., ω_{ca}, and the driving field frequency ν is denoted by Δ, i.e., $\Delta=\nu-\omega_{ca}$.

B. Lower-level coupling scheme

In this scheme, a classical driving field couples the level $|c\rangle$ with the ground level $|b\rangle$ of the three-level atom [see Fig. 1(b)]. In the presence of this additional coupling of the level $|c\rangle$ with the ground level $|b\rangle$, the atomic level $|a\rangle$ spontaneously decays to the ground level $|b\rangle$. Again we assume the phase of the driving field to be undergoing phase fluctuations resulted from the finite bandwidth of the field. As in the scheme described in Sec. II A, we are interested in the study of the spontaneous-emission spectrum of the atomic level $|a\rangle$.

The Hamiltonian for the system with the lower-level coupling, in the interaction picture and under rotating-wave approximation, is given by

$$V_{\rm int}=-\hbar\Delta|c\rangle\langle c|-\hbar\left[\frac{\Omega}{2}e^{-i\phi(t)}|c\rangle\langle b|+\frac{\Omega^*}{2}e^{i\phi(t)}|b\rangle\langle c|\right], \tag{2}$$

where Ω is the induced Rabi frequency and $\phi(t)$ is the time-dependent fluctuating phase of the field driving the atomic level $|c\rangle$ and the ground level $|b\rangle$. The detuning between the atomic transition frequency of the levels $|c\rangle$ and $|b\rangle$, i.e., ω_{cb}, and the driving field frequency ν is denoted by Δ, i.e., $\Delta=\nu-\omega_{cb}$.

C. Phase-diffusion model of the driving field

Both the above Hamiltonians i.e., Eqs. (1) and (2), represent the fluctuating phase of the driving field. This fluctuating phase can be described as

$$\phi(t)=\phi(0)+\phi_1(t), \tag{3}$$

where $\phi(0)$ is a constant corresponding to the average value of the fluctuating phase and $\phi_1(t)$ is its random part. We assume that $\phi_1(t)$ is undergoing Brownian motion described by a Gaussian random process, such that $\langle\phi_1(t)\rangle=0$. These phase fluctuations can also be characterized by the following random force:

$$F(t)=\dot{\phi}_1(t), \tag{4}$$

with zero average, i.e., $\langle F(t)\rangle=0$. This corresponds to a Weiner-Levy diffusion process which leads to the Lorentzian linewidth with bandwidth D. For such processes the two-time correlation function on the interaction time scale can be taken as

$$\langle F(t)F(t')\rangle=2D\delta(t-t'). \tag{5}$$

Now on substituting the values for $\phi(t)$ from Eq. (4) the above equation yields

$$\langle\phi(t)\phi(t')\rangle=D(t+t'-|t-t'|), \tag{6}$$

which indicates it to be a stationary process. In this paper, we have assumed, for simplicity, that $\phi(0)=0$.

III. SPONTANEOUS-EMISSION SPECTRUM

The emission spectrum of the spontaneously emitted radiation from a driven atom located at $\boldsymbol{r}_0$, at some observation point $\boldsymbol{r}$, is given by the Fourier transform of the following time-time field correlation function:

$$\mathscr{F}(t,t+\tau)=\langle E^{(-)}(\boldsymbol{r},t)E^{(+)}(\boldsymbol{r},t+\tau)\rangle , \tag{7}$$

where $E^{(\pm)}$ are the positive and negative frequency parts of the total field operator, respectively. The positive frequency part of the field operator at the position $\boldsymbol{r}$, under far field approximation and for the field polarization in x direction, can be written as [13]

$$E^{(+)}(\boldsymbol{r},t)=\frac{\omega^2 \wp \sin\eta}{4\pi\epsilon_0 c^2|\boldsymbol{r}-\boldsymbol{r}_o|}\sigma_-\left(t-\frac{|\boldsymbol{r}-\boldsymbol{r}_o|}{c}\right) , \tag{8}$$

where η is the angle between the electric dipole $\wp$ and $\boldsymbol{r}$ while ω is the atomic transition frequency. This equation indicates that the positive frequency part of the field operator, which is associated with the destruction operator of the field, is proportional to the atomic state lowering operator σ_- at a retarded time. A similar expression for $E^{(-)}$ can also be obtained.

It can be seen by substituting the values for $E^{(+)}$ and $E^{(-)}$ in Eq. (7) that the two-time correlation function of the field operators is proportional to the two-time correlation function of the atomic raising and lowering operators, i.e.,

$$\mathscr{F}(t,t+\tau)\sim\langle\sigma_+(t)\sigma_-(t+\tau)\rangle . \tag{9}$$

According to the quantum regression theorem, under certain conditions, this two-time correlation function given in Eq. (9) can be obtained from the single-time correlation function $\langle\sigma_-(t+\tau)\rangle$ [14]. As we are interested in the steady-state spectrum, i.e., $t\to\infty$, the correlation function in Eq. (9) depends on the time difference τ only and the spectrum, apart from a constant factor, will be given by

$$S(\omega;\omega_0)=\mathrm{Re}\int_0^\infty\langle\sigma_+(t)\sigma_-(t+t+\tau)\rangle_{\text{steady state}}e^{i\omega_0\tau}d\tau . \tag{10}$$

We now proceed to determine the spontaneous-emission spectra in the two atomic configurations discussed in Sec. II.

A. Upper-level coupling scheme

In this scheme, we assume that a classical field, having a finite bandwidth, is driving level $|a\rangle$ of a three-level atomic system with level $|c\rangle$ [see Fig. 1(a)]. In the presence of this additional coupling we are interested in the study of the spontaneous-emission spectrum of the atomic level $|a\rangle$ decaying to ground state $|b\rangle$. The Hamiltonian of the system is given by Eq. (1).

First we consider the expectation value of the lowering operator corresponding to the atomic transition $|b\rangle\to|a\rangle$, i.e.,

$$\langle\sigma_-(t+\tau)\rangle=\rho_{ab}(t+\tau)e^{i\omega(t+\tau)} , \tag{11}$$

where ω is the atomic transition frequency between atomic levels $|a\rangle$ and $|b\rangle$. The equation of motion for the density matrix element $\rho_{ab}(t+\tau)$ can be written in a usual way:

$$\frac{d}{dt}\rho_{ab}(t)=i\frac{\Omega^*}{2}\rho_{cb}(t)e^{i\phi(t)}-\gamma_{ab}\rho_{ab}(t) . \tag{12}$$

In the above equation, γ_{ab} is the decay rate of the off-diagonal density matrix element which is defined as follows:

$$\gamma_{ij}=\tfrac{1}{2}\sum_{k=a,b}^{c}(W_{ik}+W_{jk}) , \tag{13}$$

where W_{ij} corresponds to the population transfer from the ith level to the jth atomic level with $W_{ij}=0$ for $i=j$. It can be seen from the above equation that $\rho_{ab}(t+\tau)$ is a stochastic variable and it is coupled to $\rho_{cb}(t)e^{i\phi_1(t)}$, which is another stochastic variable. We therefore define

$$x_1(t)=\rho_{ab}(t) ,$$
$$x_2(t)=\rho_{cb}(t)e^{i\phi(t)} . \tag{14}$$

The corresponding closed set of stochastic differential equations can be written in the following matrix form:

$$\frac{d}{dt}X=[G_1+i\dot{\phi}(t)G]X , \tag{15}$$

where X is a column matrix with elements $x_1(t)$ and $x_2(t)$, and G_1 is the following time-independent matrix:

$$G_1=\begin{pmatrix}-\gamma_{ab} & i\Omega^*/2\\ i\Omega/2 & -(\gamma_{cb}-i\Delta)\end{pmatrix} . \tag{16}$$

The matrix G has just one nonzero element, i.e., $G_{22}=1$.

Next we take the ensemble average over the stochastic variable before actually solving the matrix differential equation for the required density matrix element. The resulting equation for $\langle X\rangle$ is [15]

$$\frac{d}{dt}\langle X\rangle=[G_1-DG^2]\langle X\rangle , \tag{17}$$

where, in the above equation, $\langle\,\rangle$ represents the ensemble average over the random phase $\langle\phi(t)\rangle$. The time-dependent solution of the above differential equation for the required density matrix element $\langle\rho_{ab}(t)\rangle$, i.e., $\langle x_1(t)\rangle$, is

$$\langle\rho_{ab}(t+\tau)\rangle=M_{11}(\tau)\langle\rho_{ab}(t)\rangle+M_{12}(\tau)\langle\rho_{cb}(t)e^{i\phi(t)}\rangle . \tag{18}$$

In writing the above equation, we have defined

$$M_{11}(\tau)=[e^{\bar{M}\tau}]_{11}$$
$$M_{12}(\tau)=[e^{\bar{M}\tau}]_{12} , \tag{19}$$

where $\bar{M}=G_1-DG^2$. The above value of $\langle\rho_{ab}(t+\tau)\rangle$ is then substituted in Eq. (11) to obtain the expectation value of $\langle\sigma_-(t+\tau)\rangle$, i.e.,

$$\langle\langle\sigma_-(t+\tau)\rangle\rangle=[M_{11}(\tau)\langle\rho_{ab}(t)\rangle+M_{12}(\tau)\times\langle\rho_{cb}(t)e^{i\phi(t)}\rangle]e^{i\omega(t+\tau)} . \quad (20)$$

Here the second angular bracket corresponds to the quantum-mechanical expectation value.

According to the quantum regression theorem, the evaluation of the two-time correlation function $\langle\langle\sigma_+(t)\sigma_-(t+\tau)\rangle\rangle$ is identical to the evaluation of the expectation value $\langle\langle\sigma_-(t+\tau)\rangle\rangle$ except that, instead of using $\rho(t+\tau)$, we have to use $\rho(t+\tau)\sigma_+$ [14]. Hence it follows from Eq. (20) that the two-time correlation function averaged over the stochastic process is given by

$$\langle\langle\sigma_+(t)\sigma_-(t+\tau)\rangle\rangle=[M_{11}(\tau)\langle\rho_{aa}(t)\rangle+M_{12}(\tau)\times\langle\rho_{ca}(t)e^{i\phi(t)}\rangle]e^{i\omega\tau} . \quad (21)$$

It can be seen that the two-time correlation function depends on the averages of two other stochastic variables $\rho_{aa}(t)$ and $\rho_{ca}e^{i\phi(t)}$. The differential equations corresponding to these stochastic variables can be obtained from Eq. (1) in a straightforward way, and the result is as follows:

$$\frac{d}{dt}\rho_{aa}(t)=-(W_{ac}+W_{ab}+W_{ba})\rho_{aa}(t)+i\frac{\Omega^*}{2}\rho_{ca}(t)e^{i\phi(t)} -i\frac{\Omega}{2}\rho_{ac}(t)e^{-i\phi(t)}+(W_{ca}-W_{ba})\rho_{cc}(t)+W_{ba} , \quad (22)$$

$$\frac{d}{dt}[\rho_{ca}(t)e^{i\phi(t)}]=i\frac{\Omega}{2}\rho_{aa}(t)-[\gamma_{ca}-i\Delta-i\dot{\phi}(t)]\times\rho_{ca}(t)e^{i\phi(t)}-i\frac{\Omega}{2}\rho_{cc}(t) . \quad (23)$$

In writing the above equations we have used $\rho_{bb}=1-\rho_{aa}-\rho_{cc}$. Moreover, appropriate incoherent population transfer rates, i.e., W_{ij}, are introduced. It can be seen from these equations that the required stochastic variables are coupled with other stochastic variables as well.

We can write a closed set of stochastic differential equations to obtain the solution for the required variables. For this purpose we define the variables

$$\begin{aligned} x_3(t)&=\rho_{aa}(t) ,\\ x_4(t)&=\rho_{ca}(t)e^{i\phi(t)} ,\\ x_5(t)&=\rho_{ac}(t)e^{-i\phi(t)} ,\\ x_6(t)&=\rho_{cc}(t) . \end{aligned} \quad (24)$$

The coupled set of stochastic differential equations can now be written in the following form of a stochastic matrix differential equation:

$$\frac{d}{dt}R_1=[N_1+i\dot{\phi}(t)N]R_1+I , \quad (25)$$

where R_1 is a column matrix with elements $x_3(t)$, $x_4(t)$, $x_5(t)$, and $x_6(t)$. The matrix N_1 is of the form

$$N_1=\begin{pmatrix} -\gamma_1 & i\Omega^*/2 & -i\Omega/2 & \beta_2 \\ i\Omega/2 & -(\gamma_{ca}-i\Delta) & 0 & -i\Omega/2 \\ -i\Omega^*/2 & 0 & -(\gamma_{ac}+i\Delta) & i\Omega^*/2 \\ \beta_1 & -i\Omega^*/2 & i\Omega/2 & -\gamma_2 \end{pmatrix} , \quad (26)$$

and matrices N and I have the following nonzero elements:

$$N_{22}=1, \quad N_{33}=-1, \quad I_1=W_{ba}, \quad I_4=W_{bc} . \quad (27)$$

In writing the closed set of differential equations above, we have defined the quantities

$$\begin{aligned} \gamma_1&=W_{ab}+W_{ac}+W_{ba} ,\\ \gamma_2&=W_{ca}+W_{cb}+W_{bc} ,\\ \beta_1&=W_{ac}-W_{bc} ,\\ \beta_2&=W_{ca}-W_{ba} . \end{aligned} \quad (28)$$

The stochastic averaging of the above stochastic differential equation, i.e., Eq. (35), yields the following simple inhomogeneous differential equation [15]:

$$\frac{d}{dt}\langle R_1\rangle=[N_1-DN^2]\langle R_1\rangle+I . \quad (29)$$

The net effect of the finite linewidth D of the driving field appears to be a replacement of γ_{ca} and γ_{ac} by $\gamma_{ca}+D$ and $\gamma_{ac}+D$, respectively. This is, however, a more complicated dependence than a simple rescaling as γ_1 and γ_2 [see Eq. (28)] also contain the decay and incoherent pumping rates that are contained in γ_{ca} and γ_{ac} [see Eq. (13)].

It follows from Eq. (10) that the Fourier transfer of the two-time correlation function, i.e., Eq. (21), gives the spontaneous-emission spectrum. The spectrum in the steady state can be obtained by taking the limit, $t\rightarrow\infty$, and we obtain

$$S_U(\omega_0;\omega)=\mathrm{Re}\{[\tilde{M}^{-1}(\omega_0;\omega)]_{11}\langle x_3(\infty)\rangle +[\tilde{M}^{-1}(\omega_0;\omega)]_{12}\langle x_4(\infty)\rangle\} , \quad (30)$$

where

$$\tilde{M}(\omega_0;\omega)=\begin{pmatrix} i(\omega_0-\omega)+\gamma_{ab} & -i\Omega^*/2 \\ -i\Omega/2 & i(\omega_0-\omega)+(\gamma_{cb}+D)-i\Delta \end{pmatrix} . \quad (31)$$

The required cofactors of the above matrix can be written in the following form:

$$[\tilde{M}^{-1}(\omega_0;\omega)]_{11}=\frac{1}{x-y}\left\{\frac{x-\Gamma_{cb}}{[i(\omega_0-\omega)+x]}-\frac{y-\Gamma_{cb}}{[i(\omega_0-\omega)+y]}\right\}, \quad (32)$$

$$[\tilde{M}^{-1}(\omega_0;\omega)]_{12}=\frac{-i\Omega^*}{2(x-y)}\left\{\frac{1}{[i(\omega_0-\omega)+x]}-\frac{1}{[i(\omega_0-\omega)+y]}\right\}, \quad (33)$$

where we have defined

$$x,y=\frac{(\gamma_{ab}+\Gamma_{cb})\pm\sqrt{(\gamma_{ab}-\Gamma_{cb})^2-|\Omega|^2}}{2}, \quad (34)$$

with

$$\Gamma_{cb}=(\gamma_{cb}+D)-i\Delta . \quad (35)$$

The steady-state value of the variables $\langle x_3(\infty)\rangle$ and $\langle x_4(\infty)\rangle$ appearing in Eq. (30) can be obtained by taking all the time derivatives in Eq. (29) to be zero. This gives

$$\langle x_3(\infty)\rangle=\frac{1}{\Pi_1}\left\{|\Gamma_{ac}|^2(\gamma_2 W_{ba}+\beta_2 W_{bc})+\frac{|\Omega|^2}{2}(\gamma_{ac}+D)\times(W_{ba}+W_{bc})\right\}, \quad (36)$$

$$\langle x_4(\infty)\rangle=\frac{1}{\Pi_1}\left\{i\frac{\Omega}{2}\Gamma_{ac}[(\gamma_2-\beta_1)W_{ba}+(\beta_2-\gamma_1)W_{bc}]\right\}, \quad (37)$$

where we have defined the quantities

$$\Gamma_{ac}=(\gamma_{ac}+D)-i\Delta , \quad (38)$$

$$\Pi_1=(\gamma_1\gamma_2-\beta_1\beta_2)|\Gamma_{ac}|^2+\frac{|\Omega|^2}{2}(\gamma_1+\gamma_2-\beta_1-\beta_2)\times(\gamma_{ac}+D) . \quad (39)$$

On substituting the values of $\langle x_3(\infty)\rangle$ and $\langle x_4(\infty)\rangle$ from Eqs. (36) and (37) and the values of $[\tilde{M}^{-1}(\omega_0;\omega)]_{11}$ and $[\tilde{M}^{-1}(\omega_0;\omega)]_{12}$ from Eqs. (32) and (33) into Eq. (30), and on taking the Fourier transform [see Eq. (10)] we obtain the following expression for the spectrum:

$$S_U(\omega_0;\omega)=\mathrm{Re}\left[\frac{A^{(+)}}{[i(\omega_0-\omega)+x]}-\frac{A^{(-)}}{[i(\omega_0-\omega)+y]}\right], \quad (40)$$

where

$$A^{(+)}=\frac{(x-\Gamma_{cb})\langle x_3(\infty)\rangle-i\Omega^*/2\langle x_4(\infty)\rangle}{x-y}, \quad (41)$$

$$A^{(-)}\frac{(y-\Gamma_{cb})\langle x_3(\infty)\rangle-i\Omega^*/2\langle x_4(\infty)\rangle}{x-y} . \quad (42)$$

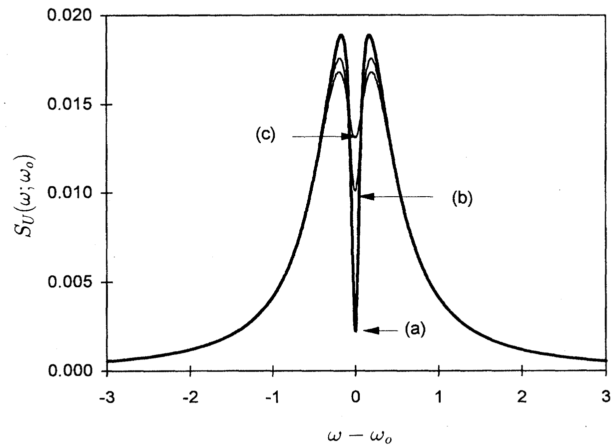

FIG. 2. Spectrum in the upper-level coupling scheme for $\Omega=0.3$ with $W_{ab}=1.0$, $W_{ba}=0.01$, $W_{ca}=0.02$ for (a) $D=0$, (b) $D=0.05$, and (c) $D=0.1$. The unit of the spectrum is W_{ab}^{-1}.

In general, both x and y are complex quantities. For large values of Ω the Stark effect complicates the above spectrum. Here in this paper we restrict ourselves to the region

$$(\gamma_{ab}-\Gamma_{cb})^2>|\Omega|^2 . \quad (43)$$

Under this condition both x and y are real and, for $\Delta=0$, the above spectrum, i.e., Eq. (40), becomes a difference of two Lorentzian functions centered at $\omega=\omega_0$ having widths equal to $2x$ and $2y$, respectively. In Fig. 2, the spectrum for the upper-level coupling scheme is shown when $W_{ab}\gg W_{ba},W_{ca},D$, under condition (43) for different values of D with $\Delta=0$. The difference of the two Lorentzian functions results in a dip at $\omega=\omega_0$ instead of a dark line as shown in Ref. [6]. It can be seen from the figure that the depth of the dip decreases with the increase in the diffusion constant D.

B. Lower-level coupling scheme

We now derive the spontaneous-emission spectrum for the second scheme where a coupling is introduced between the lower level $|b\rangle$ and the level $|c\rangle$ via a coherent driving field, having a finite bandwidth [see Fig. 1(b)]. The atom-field interaction is described by Eq. (2). In this scheme, the differential equation corresponding to the density matrix element $\rho_{ab}(t)$ is given by

$$\frac{d}{dt}\rho_{ab}(t)=-i\frac{\Omega}{2}\rho_{ac}(t)e^{-i\phi(t)}-\gamma_{ab}(t) . \quad (44)$$

As before, this is a stochastic differential equation. Let us define

$$y_1(t)=\rho_{ab}(t) ,$$
$$y_2(t)=\rho_{ac}(t)e^{-i\phi(t)} . \quad (45)$$

The corresponding closed set of stochastic differential equations is averaged over the stochastic process and the time-dependent solution for the required density matrix element is

$$\langle \rho_{ab}(t+\tau)\rangle = Z_{11}\langle \rho_{ab}(t)\rangle + Z_{12}\langle \rho_{ac}(t)e^{-i\phi(t)}\rangle \ , \quad (46)$$

where the coefficients in the above equation are defined as follows:

$$Z_{11} = [e^{\bar{Z}\tau}]_{11} \ ,$$
$$Z_{12} = [e^{\bar{Z}\tau}]_{12} \ , \quad (47)$$

with $\bar{Z} = (K_1 - DK^2)$. Here K_1 is a constant matrix of the following form:

$$K_1 = \begin{pmatrix} -\gamma_{ab} & -i\Omega/2 \\ -i\Omega^2/2 & -(\gamma_{ac}+i\Delta) \end{pmatrix} \ , \quad (48)$$

and the matrix K has just one nonzero element, i.e., $K_{22}=1$.

It follows, on substituting the average value for the density matrix element $\langle \rho_{ab}(t+\tau)\rangle$ to obtain the expectation value for the $\langle \sigma_-(t+\tau)\rangle$ and again using the quantum regression theorem, we obtain

$$\langle\langle \sigma_+(t)\sigma_-(t+\tau)\rangle\rangle = [Z_{11}(\tau)\langle \rho_{aa}(t)]e^{i\omega\tau} \ . \quad (49)$$

It is interesting to note that the two-time correlation function in this scheme just depends on $\langle \rho_{aa}(t)\rangle$, whereas in the previous scheme it depended on $\langle \rho_{ca}(t)e^{i\phi(t)}\rangle$ as well.

We recall that the real part of the Fourier transform of the two-time correlation function, Eq. (46), gives the spontaneous-emission spectrum. In the steady state, the spectrum becomes

$$S_L(\omega_0;\omega) = \mathrm{Re}\{[\tilde{Z}^{-1}(\omega_0;\omega)]_{11}\langle y_3(\infty)\rangle\} \ , \quad (50)$$

where

$$\tilde{Z}(\omega_0;\omega) = \begin{pmatrix} i(\omega_0-\omega)+\gamma_{ab} & i\Omega/2 \\ i\Omega^*/2 & i(\omega_0-\omega)+(\gamma_{ac}+D)+i\Delta \end{pmatrix} \ , \quad (51)$$

and the required cofactor of the above matrix can be written as

$$[\tilde{Z}^{-1}(\omega_0;\omega)]_{11} = \frac{1}{u-v}\left\{ \frac{u-\Gamma_{ac}}{[i(\omega_0-\omega)+u]} - \frac{v-\Gamma_{ac}}{[i(\omega_0-\omega)+v]} \right\} \ , \quad (52)$$

where we have defined

$$u,v = \frac{(\gamma_{ab}+\Gamma_{ac}) \pm \sqrt{(\gamma_{ab}-\Gamma_{ac})^2 - |\Omega|^2}}{2} \ , \quad (53)$$

with

$$\Gamma_{ac} = (\gamma_{ac}+D)+i\Delta \ . \quad (54)$$

The differential equation for the density matrix element $\rho_{aa}(t)$ is again derived for this scheme and the appropriate decay and pumping mechanisms are introduced, i.e.,

$$\frac{d}{dt}\rho_{aa}(t) = -\gamma_1\rho_{aa}(t) + \beta_2\rho_{cc}(t) + W_{ba} \ . \quad (55)$$

It can be seen here that $\rho_{aa}(t)$ is not directly coupled to the driving field. It is important to note that the pumping in atomic level $|a\rangle$ is through incoherent means from the level $|c\rangle$ which is coupled to the lower level $|b\rangle$ via the classical driving field having a finite bandwidth D. The density matrix element $\rho_{cc}(t)$ is coupled to two other stochastic variables, i.e., $\rho_{cb}(t)e^{i\phi(t)}$ and $\rho_{bc}(t)e^{-i\phi(t)}$. We therefore define the variables

$$y_3(t) = \rho_{aa}(t) \ ,$$
$$y_4(t) = \rho_{cc}(t) \ ,$$
$$y_5(t) = \rho_{cb}(t)e^{i\phi(t)} \ ,$$
$$y_6(t) = \rho_{bc}(t)e^{-i\phi(t)} \ . \quad (56)$$

The corresponding coupled set of stochastic differential equations can be written in the matrix form

$$\frac{d}{dt}R_2 = [L_1 + i\dot{\phi}(t)L]R_2 + J \ , \quad (57)$$

where R_2 is a column matrix with elements $y_3(t)$, $y_4(t)$, $y_5(t)$, and $y_6(t)$. The matrix L_1 is of the form

$$L_1 = \begin{pmatrix} -\gamma_1 & \beta_2 & 0 & 0 \\ \beta_1 & -\gamma_2 & -i\Omega^*/2 & i\Omega/2 \\ -i\Omega/2 & -i\Omega & -(\gamma_{cb}-i\Delta) & 0 \\ i\Omega^*/2 & i\Omega^* & 0 & -(\gamma_{cb}+i\Delta) \end{pmatrix} \ , \quad (58)$$

and the nonzero elements of matrix L are $L_{33}=1$, $L_{44}=-1$. The column matrix J is of the form

$$J = \begin{pmatrix} W_{ba} \\ W_{bc} \\ i\Omega/2 \\ -i\Omega^*/2 \end{pmatrix} \ . \quad (59)$$

As before, Eq. (54) is averaged over the stochastic process and solved for the steady-state value for the required variable

$$\langle y_3(\infty)\rangle = \frac{1}{\Pi_2}\left\{ |\Gamma_{bc}|^2(\gamma_2 W_{ba} + \beta_2 W_{bc}) + \frac{|\Omega|^2}{2}(\gamma_{bc}+D) \times (W_{ba}+W_{ca}) \right\} \ , \quad (60)$$

where

$$\Gamma_{bc} = (\gamma_{cb}+D)+i\Delta \ , \quad (61)$$

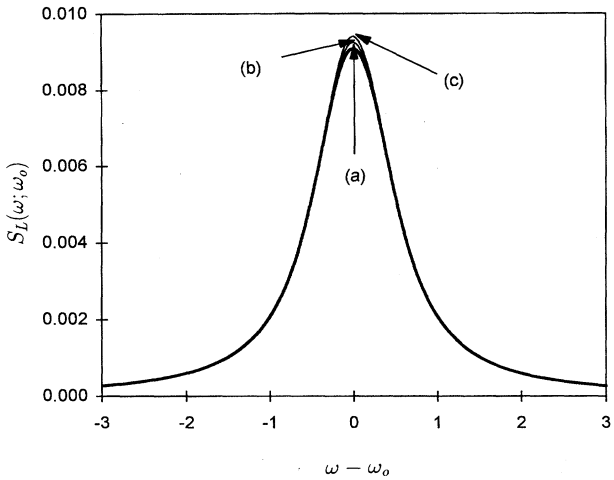

FIG. 3. Spectrum of the lower-level coupling scheme for $\Omega=0.3$ with $W_{ab}=1.0$, $W_{ba}=0.01$, $W_{cb}=0.02$ for (a) $D=0$, (b) $D=0.05$, and (c) $D=0.1$. The unit is W_{ab}^{-1}.

$$\Pi_2=(\gamma_1\gamma_2-\beta_1\beta_2)|\Gamma_{bc}|^2+\frac{|\Omega|^2}{2}(2\gamma_1+\beta_2)(\gamma_{cb}+D) . \tag{62}$$

On substituting the value of $\langle y_3(\infty)\rangle$ in Eq. (47) and using Eq. (49), we obtain the following spontaneous-emission spectrum for the lower-level coupling scheme:

$$S_L(\omega_0;\omega)=\mathrm{Re}\left[\frac{\langle y_3(\infty)\rangle}{(u-v)}\left\{\frac{u-\Gamma_{ac}}{[i(\omega_0-\omega)+u]}-\frac{v-\Gamma_{ac}}{[i(\omega_0-\omega)+v]}\right\}\right] . \tag{63}$$

The above spectrum is a difference of two Lorentzian functions under

$$(\gamma_{ab}-\Gamma_{ac})^2>|\Omega|^2 , \tag{64}$$

as both u and v are real for $\Delta=0$. The two Lorentzian functions are centered at $\omega=\omega_0$ with widths $2u$ and $2v$, respectively. In Fig. 3, the spectrum for the lower-level coupling scheme is shown for different values of diffusion constant D. For the sake of comparison, we have taken $W_{ab}\gg W_{ba}, W_{cb}, D$. It can be seen from the figure that there is no dip as there was in the case of the upper-level coupling scheme. However, for the values of parameters considered in Fig. 3, the condition (64) is no longer valid. Hence the spectrum given by Eq. (63) cannot be described as a difference of two Lorentzian functions.

We now present a comparative study of the spectra in the two coupling schemes to explain the difference, in particular, the additional dip at $\omega-\omega_0$ in the upper-level coupling scheme. We further discuss the role of incoherent pumping and finite bandwidth of the driving field on the spectrum which lead to the dip instead of a dark line in the upper-level coupling scheme [6].

IV. RESULTS AND DISCUSSION

In Ref. [6], it was shown that there exists a dark line in the spectrum of the upper-level coupling scheme for $\Delta=0$ at $\omega_0=\omega$. No such dark line exists in the lower driven case. The existence of the dark line is a consequence of quantum interference. Physically we can understand this behavior easily in the dressed atom picture. In the upper coupling case, the upper level is split in a doublet with a spacing Ω. The coherence in these levels leads to a destructive interference in the spontaneous emission at $\omega=\omega_0$, thus resulting in a dark line. On the other hand, in the lower coupling case, the lower level is split in a doublet. The spontaneous emission from the upper level to this doublet is incoherent and the resulting spontaneous-emission spectrum consists of a sum of two Lorentzians. This causes a dip at $\omega=\omega_0$, for large values of induced Rabi frequency Ω, but not a dark line. The analysis of Ref. [6], however, assumed the atom to be initially in level $|a\rangle$ and ignored any pumping mechanism, level decays, and the linewidth of the driving field. The spectra for the two cases (upper- and lower-level couplings) derived in Sec. III include all these effects. The spectrum in the two coupling schemes, i.e., Eqs. (40) and (63), reduces to the following form in the absence of any driving field (i.e., for $\Omega=0$):

$$S_{U,L}(\omega_0;\omega)=\frac{\gamma_2W_{ba}+\beta_2W_{bc}}{(\gamma_1\gamma_2-\beta_1\beta_2)}\left[\frac{\gamma_{ab}}{(\omega_0-\omega)^2+\gamma_{ab}^2}\right] . \tag{65}$$

This is a Lorentzian function centered at $\omega=\omega_0$ with a width $2\gamma_{ab}$. In the following we discuss the two spectra for the small values of induced Rabi frequencies Ω of the driving field, having finite bandwidth, in the presence of incoherent pumpings.

Let us consider the spectrum for the upper-level coupling scheme, i.e., Eq. (40), when only W_{ab}, W_{ba}, and W_{ca} are nonzero. For this case the condition (43) simplifies to

$$\tfrac{1}{4}[W_{ab}-(W_{ca}+2D)]^2>|\Omega|^2 . \tag{66}$$

The widths of the two Lorentzian functions appearing in Eq. (40) become

$$\mu_x\approx W_{ab}+W_{ba}-\frac{|\Omega|^2}{W_{ab}-(W_{ca}+2D)} , \tag{67}$$

$$\mu_y\approx W_{ba}+(W_{ca}+2D)+\frac{|\Omega|^2}{W_{ab}-(W_{ca}+2D)} , \tag{68}$$

where μ_x and μ_y are the widths of the first and second Lorentzian functions, respectively, under condition (60). It can be seen from Eq. (65) that the width of a single Lorentzian function, for this case, in the absence of driving field is $W_{ab}+W_{ba}$. As W_{ab} corresponds to the atomic decay whereas W_{ba} corresponds to incoherent pumping, we always have $W_{ab}>W_{ba}$. A comparison with the first Lorentzian function in the presence of the driving field shows that there is a slight reduction in the width. However, this reduction is accompanied by the subtraction of another Lorentzian function with width μ_y. Furthermore, for $W_{ab}>W_{ca}+D$, it can be noticed that $\mu_x>\mu_y$.

In Fig. 2, the spectrum for upper-level coupling is shown for $W_{ab} \gg W_{ba}, W_{ca}, D$, for different values of D. The subtraction of the two Lorentzian functions leads to the dip in the spectrum at $\omega = \omega_0$ as both the functions peak at this point. The width of the dip depends on the width of the second Lorentzian function, i.e., μ_y. It can be seen from Eqs. (67) and (68) that, for this particular case, we have $\mu_y \ll \mu_x$. The width of the second Lorentzian function increases with the increase in the values of W_{ba}, W_{ca}, and D [see Eq. (68)]. However, the depth of the dip depends on the difference in the values of two Lorentzian functions at $\omega = \omega_0$. In the upper-level coupling scheme, the ratio of the values of two Lorentzian functions at $\omega = \omega_0$ is [see Eq. (40)]

$$R_U = \frac{yA^{(+)}}{xA^{(-)}} . \tag{69}$$

In Fig. 4 this ratio is plotted against induced Rabi frequency Ω under the condition (66) with the same values of incoherent pumping rates as in Fig. 2, for different values of diffusion constant D. It can be seen that the ratio always remains larger than unity. This means that the contribution from the first Lorentzian function in Eq. (40) is always larger than the second Lorentzian function, which has a narrower width. Hence the difference of the two Lorentzian functions results in a dip at $\omega - \omega_0$ instead of a dark line predicted in Ref. [6]. The depth of the dip increases with Ω as it can be seen from Fig. 4 that the ratio R_U approaches unity for higher values of Ω, allowed under condition (66). The ratio, however, increases for higher values of diffusion constant D, which results in the further reduction of the depth of the dip.

For the lower-level coupling scheme, for a corresponding simple case when only W_{ab}, W_{ba}, and W_{cb} are nonzero, the condition (64) becomes

$$\tfrac{1}{4}[W_{ba} - (W_{cb} + 2D)]^2 > |\Omega|^2 . \tag{70}$$

The widths of the first and second Lorentzian functions, respectively, under the above condition are

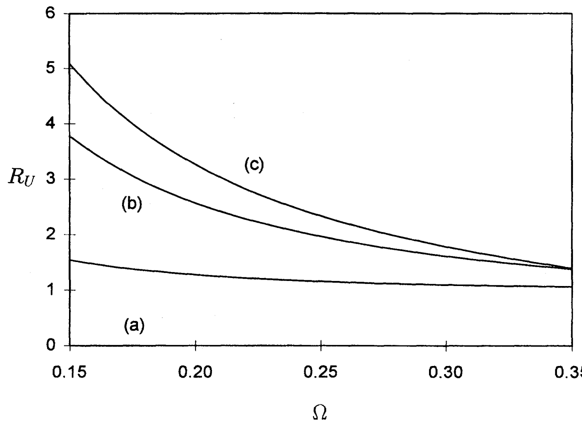

FIG. 4. The ratio of the values of two Lorentzian functions at $\omega = \omega_0$ appearing in the expression for the spectrum in the upper-level coupling scheme, i.e., Eq. (40), for the same values of incoherent pumpings as in Fig. 2 against the induced Rabi frequency Ω for (a) $D = 0$, (b) $D = 0.05$, and (c) $D = 0.1$.

$$\mu_u \approx W_{ab} + W_{ba} - \frac{|\Omega|^2}{W_{ba} - (W_{cb} + 2D)} , \tag{71}$$

$$\mu_v \approx W_{ab} + (W_{cb} + 2D) + \frac{|\Omega|^2}{W_{ba} - (W_{cb} + 2D)} . \tag{72}$$

The widths of the two Lorentzian functions are approximately equal for $W_{ab} \gg W_{ba}, W_{cb}, D$. However, the condition (70) is not satisfied for the set of parameters considered in Fig. 3. In this case both u and v given by Eq. (53) become complex and the spectrum for the lower coupling scheme cannot be described as a difference of two Lorentzian functions located at $\omega = \omega_0$. The actual form of the spectrum is more complicated, but at $\omega = \omega_0$ the contribution from the other terms vanishes and the spectrum is effectively the sum of two Lorentzian functions, i.e.,

$$S_L(\omega;\omega_0) = \frac{\langle y_3(\infty)\rangle \Gamma_{ac}}{2} \left[\frac{1}{[(\omega_0 - \omega) + \frac{1}{2}\sqrt{|\Omega|^2 - (\gamma_{ab} - \Gamma_{ac})}]^2 + \frac{1}{4}(\gamma_{ab} + \Gamma_{ac})} + \frac{1}{[(\omega_0 - \omega) - \frac{1}{2}\sqrt{|\Omega|^2 - (\gamma_{ab} - \Gamma_{ac})}]^2 + \frac{1}{4}(\gamma_{ab} + \Gamma_{ac})} \right] , \tag{73}$$

located symmetrically around $\omega = \omega_0$. For the case under discussion the two Lorentzian functions are located at

$$\omega_0 - \omega = \pm \tfrac{1}{2}\sqrt{|\Omega|^2 - \tfrac{1}{2}[W_{ba} - (W_{cb} + 2D)]} , \tag{74}$$

with equal widths $W_{ab} + \frac{1}{2}[W_{ba} + (W_{cb} + 2D)]$.

From the above discussion it can be seen that the spectrum in the upper-level coupling scheme for $W_{ab} \gg W_{ba}, W_{ca}, D$, under condition (66), is a difference of two Lorentzian functions with much narrower width of the second Lorentzian function. The presence of the incoherent pumping and finite bandwidth of the driving field in our realistic system results in a dip at $\omega = \omega_0$ instead of a dark line predicted in Ref. [6]. On the other hand, for the corresponding case in the lower-level coupling scheme, i.e., $W_{ab} \gg W_{ba}, W_{cb}, D$, the spectrum at $\omega = \omega_0$ effectively is the sum of two Lorentzian functions located around $\omega = \omega_0$. This may be attributed to the Stark splitting of the ground state $|b\rangle$.

[1] See, for example, W. H. Louisell, *Quantum Statistical Properties of Radiation* (Wiley, New York, 1973).
[2] I. Burshtein, Zh. Éksp. Teor. Fiz. **48**, 850 (1965) [Sov. Phys. JETP **21**, 567 (1965)]; M. Newstein, Phys. Rev. **167**, 89 (1968); B. R. Mollow, *ibid.* **188**, 1969 (1969).
[3] L. M. Narducci, M. O. Scully, G.-L. Oppo, P. Ru, and J. R. Tredicce, Phys. Rev. A **43**, 3748 (1991).
[4] D. J. Gauthier, Y. Zhu, and T. W. Mossberg, Phys. Rev. Lett. **66**, 2460 (1991).
[5] S. H. Autler and C. H. Townes, Phys. Rev. **100**, 703 (1955). See also P. L. Knight and P. W. Milonni, Phys. Rep. **66**, 23 (1980).
[6] S.-Y. Zhu and M. O. Scully, Phys. Lett. A **201**, 85 (1995); S.-Y. Zhu, L. M. Lorenz, and M. O. Scully, Phys. Rev. A (to be published).
[7] G. Alzetta, A. Gozzini, L. Moi, and G. Orriols, Nuovo Cimento B **36**, 5 (1976); H. R. Gray, R. M. Whitley, and C. R. Stroud, Jr., Opt. Lett. **3**, 218 (1978).
[8] M. O. Scully, Phys. Rev. Lett. **55**, 2802 (1975); M. O. Scully and M. S. Zubairy, Phys. Rev. A **35**, 752 (1987); W. Schleich and M. O. Scully, *ibid.* **37**, 1261 (1987); J. Bergou, M. Orszag, and M. O. Scully, *ibid.* **38**, 754 (1988); K. Zaheer and M. S. Zubairy, *ibid.* **38**, 5227 (1988).
[9] O. Kocharovskaya and Ya. I. Khanin, JETP. Lett. **48**, 630 (1988); S. E. Harris, Phys. Rev. Lett. **62**, 1033 (1989); M. O. Scully, S.-Y. Zhu, and A. Gavrielides, *ibid.* **62**, 2813 (1989); O. Kocharovskaya and P. Mandel, Phys. Rev. A **42**, 523 (1990).
[10] S. E. Harris, J. E. Field, and A. Imamoglu, Phys. Rev. Lett. **64**, 1107 (1990); K. Hakuta, L. Marmet, and B. R. Stoicheff, *ibid.* **66**, 596 (1991); K. J. Boller, A. Imamoglu, and S. E. Harris, *ibid.* **67**, 3062 (1991); J. E. Field, K. H. Hahn, and S. E. Harris, *ibid.* **67**, 3062 (1991).
[11] M. O. Scully, Phys. Rev. Lett. **67**, 1855 (1991); M. O. Scully and M. Fleischhauer, *ibid.* **69**, 1360 (1992).
[12] S. Sultana and M. S. Zubairy, Phys. Rev. A **49**, 438 (1994).
[13] See, for example, M. O. Scully, and M. S. Zubairy, *Quantum Optics* (Cambridge University Press, Cambridge, England, in press).
[14] See for example, M. Sargent III, M. O. Scully, and W. E. Lamb, Jr., *Laser Physics* (Addison-Wesley, Reading, MA, 1974).
[15] R. F. Fox, J. Math. Phys. **13**, 1196 (1972); J. Gea-Banacloche and M. S. Zubairy, Phys. Rev. A **42**, 1742 (1990).